ChemBioChem

Research Article
doi.org/10.1002/cbic.202300670

Chemistry Europe
European Chemical Societies Publishing

www.chembiochem.org

Special Collection

Targeted Preparation and NMR Spectroscopic Characterization of Lys11-Linked Ubiquitin Trimers

Fabian Immler,[a] Tobias Schneider,[a] and Michael Kovermann*[a]

Ubiquitylation refers to the attachment of mono- or polyubiquitin molecules to a substrate protein. To shield ubiquitin chains against potential hydrolysis, a facile, click-chemistry based approach was recently established for the generation of site-specifically conjugated ubiquitin dimers relying on triazole-linkage. Here, the preparation of such ubiquitin chains was advanced by the generation of homotypic Lys11-linked ubiquitin trimers considering an isotopic labeling scheme in a moiety-wise manner. The structural and dynamical impact on the ubiquitin unit at proximal, central, or distal position that is potentially invoked by the respective other two moieties was systematically probed by heteronuclear high-resolution NMR spectroscopic approaches. As a result, conjugating a third ubiquitin moiety to the proximal or distal site of a ubiquitin dimer does not alter structural and dynamical characteristics as it has been seen for ubiquitin dimers. This observation suggests that recognition of a homotypically assembled ubiquitin chain by a potential substrate is primarily done by screening the length of a ubiquitin chain rather than relying on subtle changes in structure or dynamic properties of single ubiquitin moieties composing the chain.

By changing interaction surfaces and binding properties post-translational modifications (PTMs) act as a common mechanism for modulating and regulating protein function. In eukaryotes, a large variety of PTMs are known, including phosphorylation, acetylation, methylation, ubiquitylation, sumoylation, neddylation, and glycosylation.[1] Ubiquitylation in particular represents one of the most prevalent PTMs and significantly enhances the structural and functional flexibility of a protein.[2] The process is defined as the attachment of a single ubiquitin (Ub) unit or a polyubiquitin (polyUb) chain to a substrate protein. The biological fate of a such modified substrate protein is determined by the length of the Ub chain as well as the respective position used for linkage,[3] enabling it to regulate many cellular processes, such as cell proliferation, protein degradation, and DNA metabolism.[4] In nature, ubiquitylation is accomplished enzymatically by forming an isopeptide bond between the C-terminus of a ubiquitin molecule and an intrinsic lysine residue of the substrate. If this also occurs at one of the seven intrinsic lysine residues (K6, K11, K27, K29, K33, K48, and K63) or the N-terminal methionine (M1) of Ub, longer polyUb chains are assembled.[2–3] Note, that the polyUb chains can either be homotypic if the same conjugation site is addressed or heterotypic if distinct sites are addressed.[5] As one Ub molecule may carry up to eight other Ub units, polyUb chains can also be branched and even form dendrimers, exponentially expanding the complexity of Ub polymers.[6] The seven lysine residues comprising Ub differ in surface area representation and show variation in solvent exposure. Thus, e.g., K63 is the linkage site most exposed to the solvent and does not form intramolecular contacts, whereas K27 is the least exposed to the solvent, pointing towards the hydrophobic core.[2]

A comprehensive proteomic analysis revealed that the various Ub linkages exist in vastly different abundances. K48- (29%), K11- (28%) and K63-linkages (16%) represent the three most abundant linkages, whereas K6- (11%), K27- (9%), K33- (4%) and K29-linkages (3%) are rather rare.[7] However, the relative composition of linkages is also depending on the specific cellular conditions. For instance, K11-linkages are upregulated when cells are stressed by proteasome inhibition, heat shock, formation of toxic aggregates, or when they pass through a specific cell cycle stage. In this phase, homogenous K11-linked chains were discovered as the product of the human E3 anaphase-promoting complex (APC/C), which is an essential regulator of cell division. When APC/C is activated during mitosis, K11-linked chains rise dramatically in abundance, conversely, when cells exit the cell cycle during differentiation, the levels of K11-linkages appear to decrease. Taken together, these discoveries show that most known K11-specific enzymes are linked to mitotic control and that homogenous K11-linked Ub chains may be important regulators of cell division in higher eukaryotes.[8] Apart from that, the same linkage is also used to mark substrates for endoplasmic reticulum-associated degradation (ERAD).[7] K27-linked Ub chains have allocated functions in mitochondrial maintenance, mitophagy, and autophagy.[9] K48-linked Ub chains act as the predominant signal for proteasomal degradation,[2–3] whereas K63-linked Ub chains are involved in

[a] F. Immler, Dr. T. Schneider, Prof. Dr. M. Kovermann
Universität Konstanz
Department of Chemistry and
Graduate School of Chemical Biology (KoRS-CB)
Universitätsstraße 10, 78457 Konstanz (Germany)
E-mail: michael.kovermann@uni-konstanz.de

Supporting information for this article is available on the WWW under https://doi.org/10.1002/cbic.202300670

This article is part of a Special Collection: Decoding the Ubiquitin System Using Chemical Biology Tools.

non-degradative processes like NF-κB activation, intracellular trafficking, or DNA damage response.[10]

The biological fate of a ubiquitylated substrate protein is realized by downstream effector proteins, usually consisting of multiple ubiquitin-binding domains (UBDs), which are able to recognize the type of Ub chain, e.g. which linkage site is addressed.[11] However, not only the site used for linkage is important for cellular signaling, but also the length of the Ub chain may play a vital role in terms of function.[12] It has been shown that in the case of K48-linked Ub chains a minimum length of four Ub moieties is required to constitute an effective signal for degradation.[12a] Another example highlighting the importance of chain length is represented by the deubiquitylating enzyme (DUB) USP5, which possesses four UBDs and binds Ub tetramers with significantly higher affinity compared to Ub dimers ($K_D^{dimer} = 2510 \pm 70$ nM, $K_D^{tetramer} = 219 \pm 8$ nM).[13] Furthermore, pulldown experiments from HEK293T whole cell lysate disclosed more than 110 binding partners of homotypically assembled K27-, K29-, and K33-linked Ub chains, with many of them showing length-dependent interaction patterns.[12e]

However, the isopeptide bond is susceptible to hydrolyzation, especially by DUBs, severely limiting the application of natively assembled Ub chains in studies aiming to identify linkage-specific binding partners.[14] To overcome this obstacle, a click-chemistry based approach has been recently established for the generation of linkage-specific Ub dimers that are connected through a non-hydrolyzable triazole-linkage.[15] This artificial linkage has similar electronic and steric properties as the native isopeptide bond and the structural and dynamical properties of respective Ub dimers do not differ significantly.[16] Thus, artificially triazole-linked Ub chains that are resistant against DUB activity represent promising candidates that can be reliably used in e.g. affinity enrichment assays.

Here, three different K11-linked homotypic Ub trimers possessing respective isotopic labeling of either the proximal, central, or distal moiety were aimed to be generated and their structural and dynamical characteristics were subsequently probed by means of high-resolution NMR spectroscopy. The Ub trimers were synthesized using the previously described approach with slight modifications.[17] Briefly, three different Ub variants representing the monomeric building blocks for the trimers were recombinantly expressed at first. The Ub variant used for the proximal moiety (UbK11C) comprises a K11C single-point mutation. The Ub variant used for the distal moiety (UbG75Aha) was obtained by deleting C-terminal G76 and replacing G75 by the unnatural amino acid azidohomoalanine (Aha) via selective pressure incorporation.[18] Finally, the Ub variant used for the central moiety of the trimer (UbK11C_G75Aha) combines both modifications, K11C mutation and insertion of Aha at the C-terminus. By following the reaction scheme presented in Figure 1A the three moieties can be concatenated in a modular manner while keeping control over the chain length. First, UbK11C was equipped with an alkyne functionality at sequence position 11 by Michael addition reaction with a propargyl acrylate (PA) linker and then conjugated with UbK11C_G75Aha by Cu(I)-catalyzed azide–alkyne cycloaddition (CuAAC).[19] Second, after purifying the resulting Ub dimer by size exclusion chromatography another PA linker was added to the free cysteine at sequence position 11 of the intended central moiety constituting the Ub trimer and then conjugated with UbG75Aha by CuAAC again. Pure K11-linked Ub trimer was then obtained after removing potential existing Ub monomer and dimer species by size-exclusion chromatography (Figure 1B, C).

To resolve the spectral degeneracy resulting from the structural similarity of the three Ub moieties comprising the trimer, domain-specific isotope labeling of either the proximal or the distal moiety was additionally applied. Thus, UbK11C and UbG75Aha were also expressed with doubly $^{13}C/^{15}N$ labeling and optionally used to assemble respective Ub trimers as outlined above. In this way, the structural properties of the individual Ub moieties can be monitored on a residue-by-residue level by applying two-dimensional (2D) ^{1}H-^{15}N heteronuclear single quantum coherence (HSQC) NMR spectroscopy (Figures S1, S2). Due to the strong congruence of the spectra, the backbone amide resonance assignments obtained from corresponding monomeric building blocks and K11-linked Ub dimer, respectively, have been transferred to the two-dimensional NMR spectra acquired on Ub trimers probed here. Then, weighted differences in chemical shift values obtained in the proton and nitrogen dimension (chemical shift perturbations, CSPs) have been determined by comparing Ub monomers, dimers, and trimers with each other. This strategy enables to precisely analyze the structural impact exerted on the respective isotopically labeled Ub moiety by adding either an additional single Ub molecule or a Ub dimer comprising the same linkage.

In detail, three clusters of residues with significant CSP values are apparent when UbK11C is compared to the proximal moiety of the K11-linked Ub dimer (Figure 2A). The corresponding residues reside (*i*) next to the conjugation site in the β1- and β2-strand and the flexible loop in between, (*ii*) at the C-terminal end of the central α-helix and (*iii*) around to the C-terminal end of the last β5-strand. As previously reported, most of these perturbations are rather the consequence of the conjugation itself than the formation of a potential interdomain interface and are also observed for the corresponding isopeptide-linked Ub dimer.[16a,20] Interestingly, especially residues that are part of the so-called TEK box (K6, K11, T12, T14, and E34) are affected, which is crucially involved in the formation of K11-linked Ub chains by APC/C in the context of cell cycle regulation.[21] This implies that the artificial triazole-linkage used in this study is capable to mirror conformational features of the native isopeptide bond that are associated with K11-specific functions.

When the same analysis is expanded to trimers, and UbK11C is compared to the proximal moiety of the K11-linked ubiquitin trimer, essentially the same CSP pattern is apparent (Figure 2B). However, direct comparison between the proximal moieties of the K11-linked Ub dimer and the trimer reveals baseline effects only (Figure 2C). This indicates that the attachment of a third Ub moiety to the distal end of the dimer has no significant structural impact on the proximal moiety and does

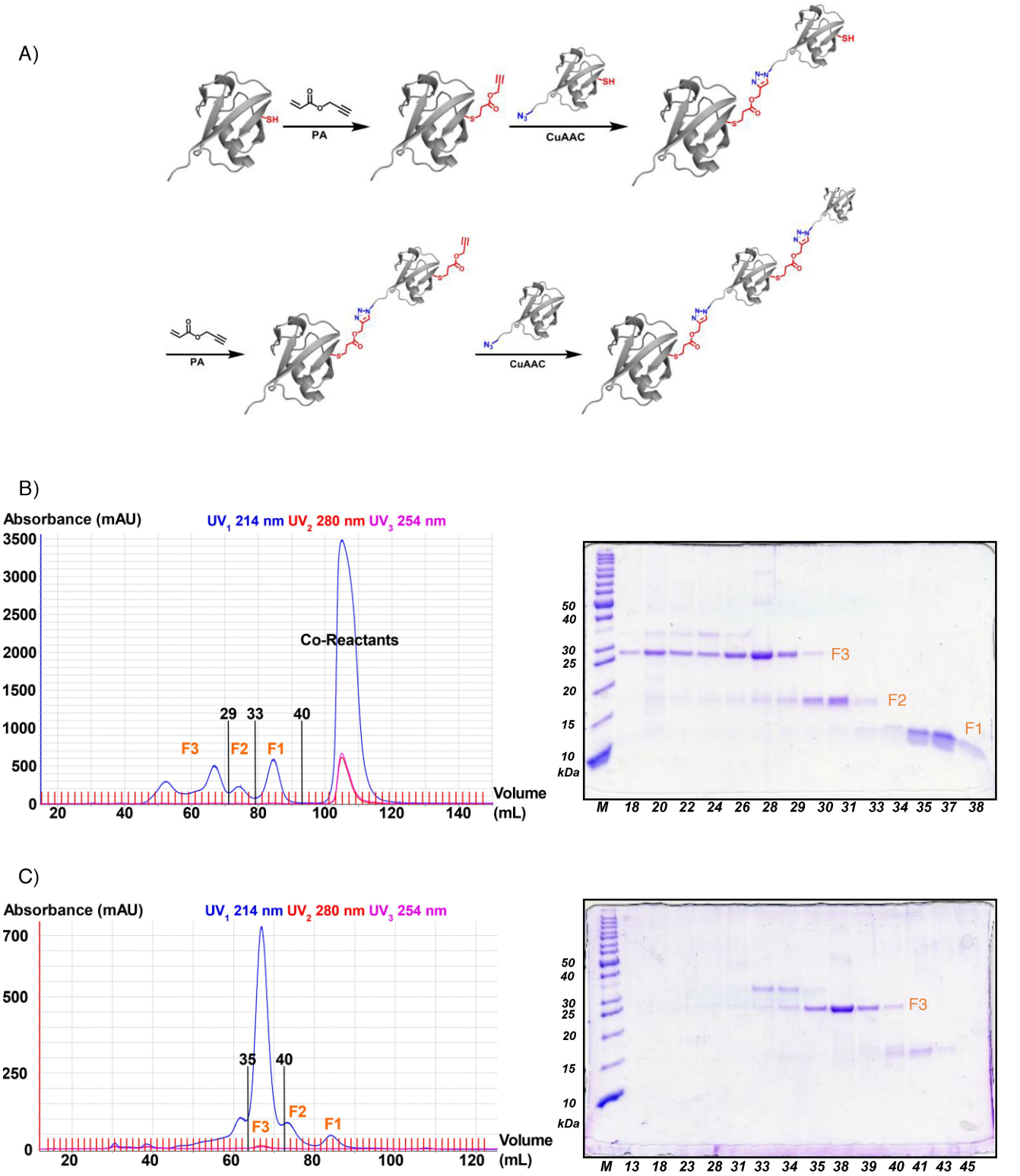

Figure 1. Targeted preparation of Ub trimers. A) Synthetic scheme for the synthesis of Ub chains of defined lengths. B) and C) Left: Chromatograms reporting on size exclusion chromatography (SEC) aiming for the purification of Ub trimer. Right: SDS-PAGE analysis of correspondingly performed SEC. Numbers displayed horizontally beneath the gel indicate corresponding fractions according to the chromatograms presented on the left (bottom). Numbers displayed vertically on the left side of the gel indicate the molecular weights of the marker 'M' that run on the first lane. To improve NMR sample purity fractions 16–29 from a first SEC run that is presented in B) were used as input for a second SEC run that is presented in C). F1 = Monomer (distal unit), F2 = Dimer-PA, and F3 = Trimer.

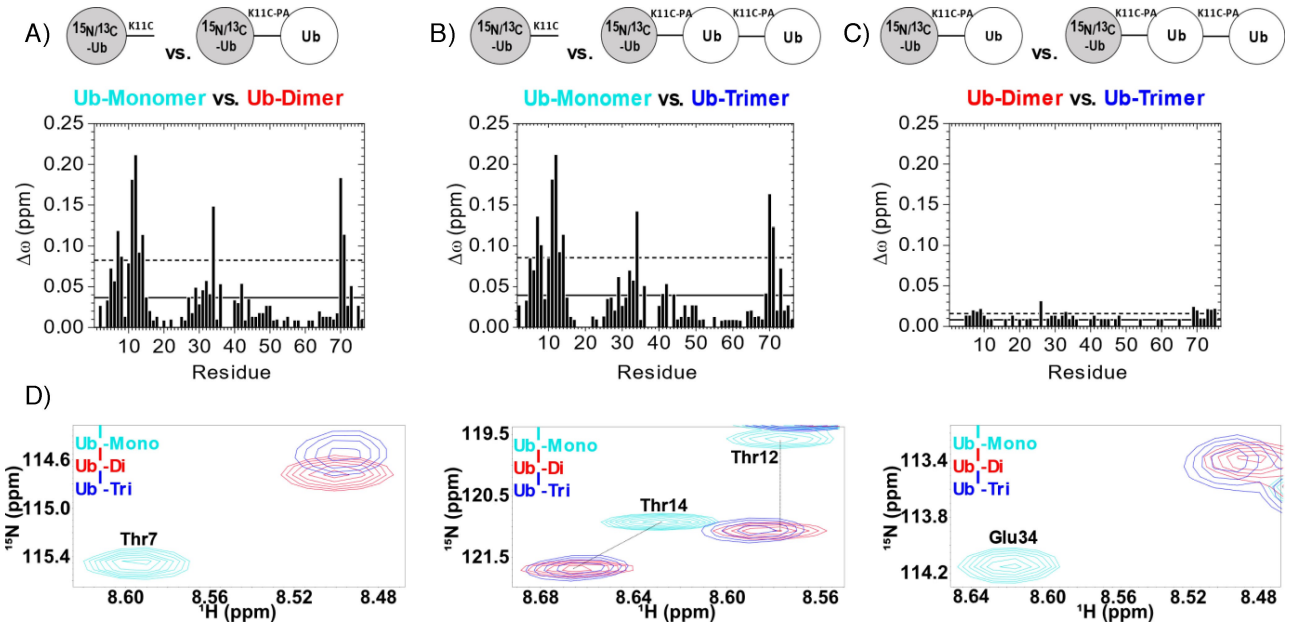

Figure 2. CSP analysis on the proximal moiety of K11-linked Ub trimer. A) Weighted chemical shift perturbations (CSPs, $\Delta\omega$,) of backbone amide resonances calculated between the proximal moiety of the triazole-linked Ub dimer assembled by using sequence position 11 as conjugation site and UbK11C, which is the corresponding monomeric building block. B) CSPs calculated between the proximal moiety of the triazole-linked Ub trimer assembled by using sequence position 11 as conjugation site and UbK11C. C) CSPs calculated between the proximal moieties of the triazole-linked Ub trimer and dimer, respectively, assembled by using sequence position 11 as conjugation site. The Ub species used for comparison are schematically depicted on top with the isotopically labeled Ub moiety colored in gray. The solid line represents the mean value of $\Delta\omega$, the dotted line is the mean value plus one standard deviation. The underlying heteronuclear ^{1}H-^{15}N HSQC NMR spectra are presented in Figure S1 and close-up views of selected cross peaks are additionally shown in D). Backbone amide resonances arising from monomeric UbK11C are colored in cyan, from the K11-linked Ub dimer are colored in red, and from the the K11-linked Ub trimer are colored in dark blue, respectively. The former ones are additionally labeled by using the one-letter code for amino acids followed by the position in the primary sequence. Note that the subscript (Roman numeral) given in the figure legend indicates the position of the Ub moiety within the assembled Ub chain that is isotopically labeled and thus exclusively apparent in the corresponding spectrum.

not interfere with the K11-specific conformational features described above.

In the next step, UbG75Aha was compared to the distal moiety of the K11-linked Ub dimer and then to the distal moiety of the respective trimer (Figure 3A, B). Again, the resulting CSP patterns are almost identical, despite the overall amplitudes of the perturbations being somewhat lower than observed in the corresponding analysis of the proximal moieties (Figure 2A, B). As CSP values of significance are exclusively found for residues located at the C-terminal tail – except for K48 – they are presumably caused by the conjugation (Figure 3A, B). Moreover, no significant perturbations are apparent when the distal moiety of the K11-linked Ub dimer is directly compared to the respective trimer (Figure 3C). Thus, it can be concluded that also the attachment of a third Ub molecule to the proximal end of the dimer does not significantly alter the conformation of the distal moiety. As neither the proximal nor the distal moiety of the trimer is capable to sense the respective moiety at the other end of the chain, a less compact conformation is proposed to be adapted by the K11-linked Ub trimer in solution (Figure 4).

Despite a low yield preventing the assembly of a K11-linked Ub trimer with domain-specific isotope labeling of the central moiety, it was feasible to prepare a doubly ^{13}C/^{15}N-labeled variant of UbK11C_G75Aha and concatenate it with unlabeled UbK11C modified with PA (Figure 1A). The resulting molecule allows to unravel the structural impact of introducing a K11C single-point mutation in the distal moiety of the K11-linked Ub dimer which is an inherent step of a potential trimer formation. Thus, a 2D ^{1}H-^{15}N HSQC NMR spectrum was acquired and corresponding CSP values were calculated with reference to K11-linked Ub dimer lacking the respective modification (Figures S3, S4 A). It was found that residues showing CSP values of significance primarily cluster next to the mutation site and with lower amplitudes at the C-terminal tail. Interestingly, subsequent PA linker attachment does not additionally invoke noticeable perturbations at the C-terminal end of the α-helix vis-à-vis to K11 as it was reported previously for the same modification on monomeric UbK11C (Figure S4B).[16a] It can be speculated that the respective conformational rearrangement in this area is hampered by the stabilization of the adjacent C-terminal tail due to the conjugation with the proximal moiety. Therefore, it seems that K11-specific structural features are more pronounced in the proximal moiety than in the central moiety of a potential Ub trimer and even longer polyUb chains.

To monitor changes in the conformational dynamics of Ub that are induced by adding one or two additional Ub moieties ^{1}H-^{15}N heteronuclear NOE spectroscopy was performed reporting on rapid backbone motions on the picosecond-to-nanosecond time scale. A respective hetNOE dataset was collected for the K11-linked Ub trimer with domain-specific isotope labeling of the proximal moiety and directly compared to the

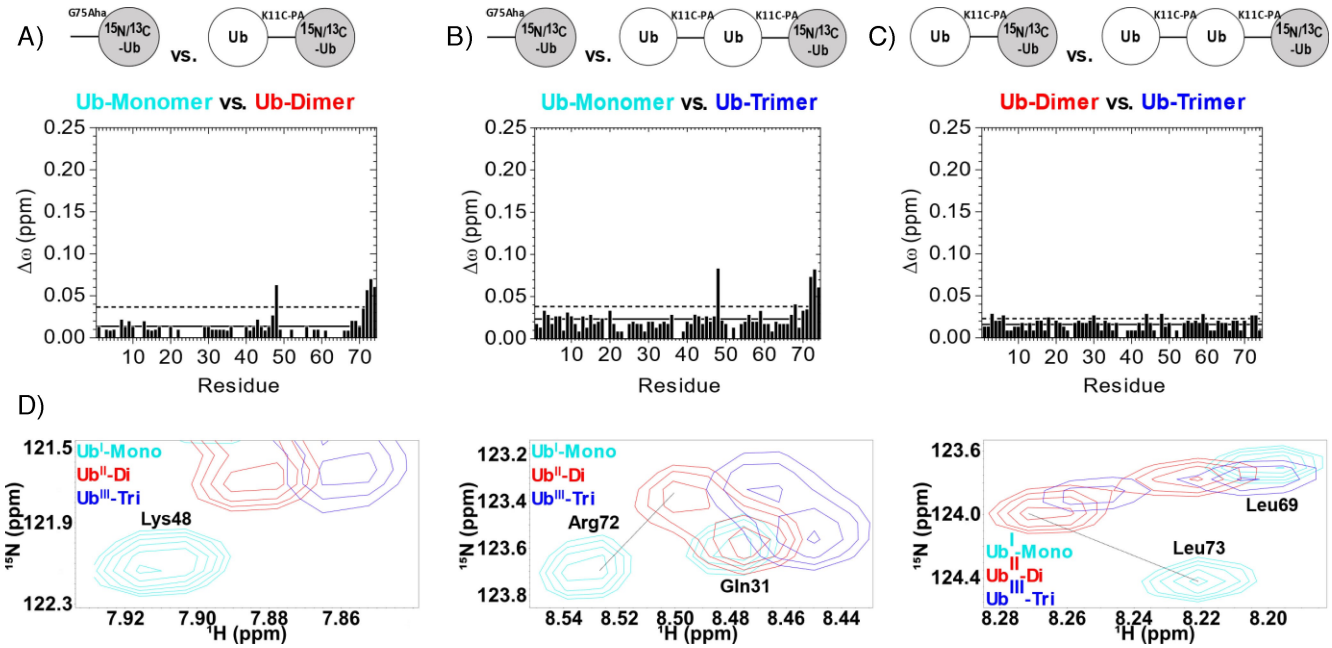

Figure 3. CSP analysis on the distal moiety of K11-linked Ub trimer. A) Weighted chemical shift perturbations (CSPs, $\Delta\omega$) of backbone amide resonances determined for the distal moiety of the triazole-linked Ub dimer assembled by using sequence position 11 as conjugation site and UbG75Aha, which represents the corresponding monomeric building block. B) CSPs calculated between the distal moiety of the triazole-linked Ub trimer assembled by using sequence position 11 as conjugation site and UbG75Aha. C) CSPs calculated between the distal moieties of the triazole-linked Ub trimer and dimer, respectively, assembled by using sequence position 11 as conjugation site. The Ub species used for comparison are schematically depicted on top with the isotopically labeled Ub moiety colored in gray. The solid line represents the mean value of $\Delta\omega$, the dotted line is the mean value plus one standard deviation. Corresponding heteronuclear ^{1}H-^{15}N HSQC NMR spectra are presented in Figure S2 and selected close-up views are shown in D). Backbone amide resonances arising from monomeric UbG75Aha are colored in cyan, from K11-linked Ub dimer are colored in red, and from K11-linked Ub trimer are colored in dark blue, respectively. The former ones are additionally labeled by using the one-letter code for amino acids followed by the position in the primary sequence. Note that the subscript (Roman numeral) indicates the position of the Ub moiety within the assembled Ub chain that is isotopically labeled and thus exclusively apparent in the corresponding NMR spectrum.

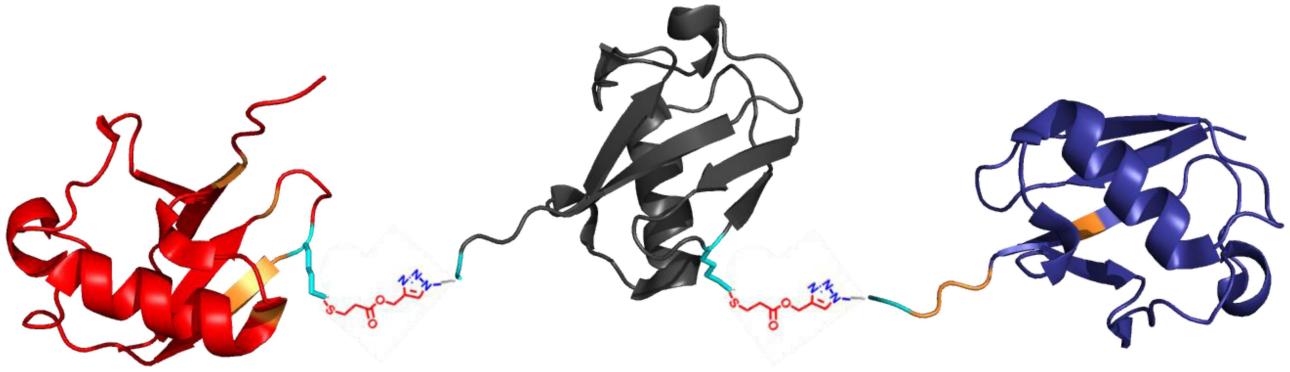

Figure 4. Conformational arrangement suggested on basis of chemical shift perturbations for a K11-linked homotypic Ub trimer. The proximal Ub moiety is colored in red, the distal moiety in blue, and the central moiety in black. Orange color indicates residues possessing CSP values of significance (values exceeding the mean plus one standard deviation/dashed line in Figure 2 (proximal moiety) and Figure 3 (distal moiety), respectively). Cyan color indicates sites used for conjugation through triazole-linkage (chemical structure shown). Note that the conformational arrangement suggested here accounts for the observation that significant CSP values are more pronounced in the proximal than in the distal moiety implying that the central moiety is potentially located somewhat closer to the former one.

corresponding Ub dimer (Figure S5). Both variants show an overall comparable pattern of individual hetNOE values and average values that are strikingly similar ($hetNOE^{mean,dimer} = 0.78 \pm 0.06$, $hetNOE^{mean,trimer} = 0.77 \pm 0.29$). Thus, the hetNOE analysis indicates that in terms of large-amplitude motions the backbone dynamics of the proximal Ub moiety within a dimer remain unaffected by the attachment of an additional Ub moiety at distal end of the chain.

In addition to the structural and dynamical analysis performed above, we also examined the hydrodynamic properties of a homotypically K11-linked Ub trimer by diffusion NMR methodology and evaluated the dependency of the diffusion coefficient on the chain length. The analysis of translational

diffusion profiles related to K11-linked Ub dimer, Ub trimer and two corresponding monomeric building blocks shows a significant decrease of the diffusion coefficient D with increasing chain length: D (K11C_G75Aha) = (13.0 ± 0.6)*10^{-11} m^2s^{-1}, D (UbK11C-PA) = (12.26 ± 0.04)*10^{-11} m^2s^{-1}, D (K11-Dimer-PA) = (9.52 ± 0.05)*10^{-11} m^2s^{-1}, D (K11-Trimer) = (8.13 ± 0.05)-*10^{-11} m^2s^{-1} (Figure S6, Table S1). These data indicate an increase in the hydrodynamic dimension of the molecule with a growing number of Ub moieties concatenated by the chemical biology approach outlined here. This observation can be also interpreted such that the overall structural arrangement does not change significantly for a K11-linked Ub chain when comparing a dimer with a trimer.

To further illuminate this finding we calculated the theoretical hydrodynamic radii, R_H, of a Ub monomer, dimer, and trimer assuming a perfectly spherical shape, following Wilkins' and coworkers' method.[22] Increasing the number of residues from N = 150 (dimer) to N = 225 (trimer) would suggest an increase in R_H by about 12%. However, experimentally we observed a change in R_H by about 17% when the Ub dimer is compared to the Ub trimer. A similar trend in the discrepancy between theoretically calculated and experimentally obtained R_H values becomes apparent if the trimer or the dimer is compared to the monomer (Table S2). On the one hand, this implies that the K11-linked Ub chains studied here are less compact than it would be expected for a properly folded protein of the same molecular size which may accounts for the dynamic nature of a multi-domain protein. On the other hand, the degree of compactness does not significantly change with an increasing chain length. Thus, based on the change in hydrodynamic dimension observed when going from a Ub dimer to a Ub trimer and from a Ub monomer to Ub dimer, respectively, we conclude that the overall conformational arrangement is inherently conserved for homotypically K11-linked Ub chains.

Taken together, we have shown a robust approach for the targeted generation of isotopically labeled Ub trimers on a milligram scale using sequence position 11 as conjugation site for homotypic linkage. Advantageously, such prepared Ub trimers possess a specific scheme of isotopic labeling enabling subsequent characterization by applying high-resolution NMR spectroscopic approaches in a moiety-wise manner. Thus, it could be shown by analyzing heteronuclear 2D ^{1}H-^{15}N HSQC NMR spectra that structural characteristics observed for the Ub moiety conjugated at the distal or proximal site forming a Ub dimer resembles features as observed when this Ub moiety is conjugated at the distal or proximal site constituting a Ub trimer. This observation suggests that the conformational ensemble of a K11-linked Ub trimer probed in thermodynamic equilibrium does not indicate prominent interactions among Ub moieties. The conservation of inherent features when the Ub trimer is compared with the corresponding Ub dimer is corroborated by analyzing backbone dynamics on the fast picosecond-to-nanosecond time scale at a residue-by-residue level while focusing again on the distal and proximal moiety comprising a trimer. We speculate, in functional consequence, that Ub chains differing in length are distinguished by respective binding partners on basis of the number of Ub moieties contributing to the interaction rather than the recognition of specific topologies adopted by the building blocks composing the chain. Previous studies have focused on the identification of UBDs and corresponding Ub binding proteins, mostly DUBs, with subsequent quantification of their interaction with Ub chains.[23] The modulation of the cellular signal that was observed upon altering the chain length was explained by a higher binding affinity when the number of UBDs increased.

By detailed structural analysis, as performed in this study by using NMR spectroscopic approaches, additional information can be obtained for a better understanding of Ub signaling processes. Thus, we expect that a profound structural analysis of longer Ub chains that are also conducted in conjunction with interaction studies will provide intimate insight into the physiological role of longer Ub chains and will illuminate the molecular basis for adaptations in functionality that go along with an increase in chain length.

Experimental Section

Synthesis of Ub trimers by click-chemistry

A sample containing proximally isotopically labeled Ub dimer (K11-Dimer-PA) was mixed with unlabeled Ub monomer (UbG75Aha) or unlabeled Ub dimer (K11-Dimer-PA) was mixed with isotopically labeled Ub monomer (UbG75Aha) in Tris·HCl (20 mM, pH 7.0) buffer. Then, SDS and THPTA with final concentrations of 0.5 mM and 5 mM, were added sequentially, followed by argon flushing. The click reaction was initiated by adding $Cu(MeCN)_4BF_4$ (2.5 mM), and samples were incubated on ice for 3 h. Subsequently, the reaction mixture was purified via size-exclusion chromatography (HiLoad 16/600 Superdex 75 pg, ÄKTA purifier FPLC system) with PBS (140 mM NaCl, 2.7 mM KCl, 10 mM Na_2HPO_4, 1.8 mM KH_2PO_4, pH 7.3) used as the elution buffer. Eluted fractions of 1.5 mL each were taken and the chromatography was tracked using SDS-PAGE analysis. Fractions containing Ub trimer were concentrated using centrifugal filters (Amicon Ultra 3 kDa MWCO) and quantified by means of BCA protein assay. Detailed protocols for expression and purification of all three Ub moieties generated in the present study and further experimental steps towards the generation of Ub trimers are given in the Supporting Information (Figure S7).

Supporting Information

This Communication is accompanied by a Supporting Information. The authors have cited additional references within the Supporting Information.[17b,22,24]

Acknowledgements

This work was supported by the DFG (SFB969, project B09). We thank the University of Konstanz for the permanent investment into the NMR infrastructure and the Konstanz Research School Chemical Biology for support. We also thank Andreas Marx and Martin Scheffner for their continuous support. Open Access funding enabled and organized by Projekt DEAL.

Conflict of Interests

The authors declare no conflict of interest.

Data Availability Statement

The data that support the findings of this study are available from the corresponding author upon reasonable request.

Keywords: click-chemistry · NMR spectroscopy · proteins · ubiquitylation

[1] A. P. Lothrop, M. P. Torres, S. M. Fuchs, *FEBS Lett.* **2013**, *587*, 1247–1257.
[2] C. Alfano, S. Faggiano, A. Pastore, *Trends Biochem. Sci.* **2016**, *41*, 371–385.
[3] D. Komander, M. Rape, *Annu. Rev. Biochem.* **2012**, *81*, 203–229.
[4] a) L. Spasser, A. Brik, *Angew. Chem. Int. Ed.* **2012**, *51*, 6840–6862; b) D. Popovic, D. Vucic, I. Dikic, *Nat. Med.* **2014**, *20*, 1242–1253.
[5] a) C. Grabbe, K. Husnjak, I. Dikic, *Nat. Rev. Mol. Cell Biol.* **2011**, *12*, 295–307; b) Y. Kravtsova-Ivantsiv, T. Sommer, A. Ciechanover, *Angew. Chem. Int. Ed.* **2013**, *52*, 192–198.
[6] M. E. French, C. F. Koehler, T. Hunter, *Cell Discovery* **2021**, *7*, 6.
[7] P. Xu, D. M. Duong, N. T. Seyfried, D. Cheng, Y. Xie, J. Robert, J. Rush, M. Hochstrasser, D. Finley, J. Peng, *Cell* **2009**, *137*, 133–145.
[8] a) K. E. Wickliffe, A. Williamson, H.-J. Meyer, A. Kelly, M. Rape, *Trends Cell Biol.* **2011**, *21*, 656–663; b) M. L. Matsumoto, K. E. Wickliffe, K. C. Dong, C. Yu, I. Bosanac, D. Bustos, L. Phu, D. S. Kirkpatrick, S. G. Hymowitz, M. Rape, *Mol. Cell* **2010**, *39*, 477–484.
[9] a) Y. Kulathu, D. Komander, *Nat. Rev. Mol. Cell Biol.* **2012**, *13*, 508–523; b) N. Birsa, R. Norkett, T. Wauer, T. E. Mevissen, H.-C. Wu, T. Foltynie, K. Bhatia, W. D. Hirst, D. Komander, H. Plun-Favreau, *J. Biol. Chem.* **2014**, *289*, 14569–14582; c) Z. Liu, P. Chen, H. Gao, Y. Gu, J. Yang, H. Peng, X. Xu, H. Wang, M. Yang, X. Liu, *Cancer Cell* **2014**, *26*, 106–120; d) V. R. Palicharla, S. Maddika, *Cell. Signalling* **2015**, *27*, 2355–2362; e) W. Kim, E. J. Bennett, E. L. Huttlin, A. Guo, J. Li, A. Possemato, M. E. Sowa, R. Rad, J. Rush, M. J. Comb, *Mol. Cell* **2011**, *44*, 325–340.
[10] S. Paiva, N. Vieira, I. Nondier, R. Haguenauer-Tsapis, M. Casal, D. Urban-Grimal, *J. Biol. Chem.* **2009**, *284*, 19228–19236.
[11] I. Dikic, S. Wakatsuki, K. J. Walters, *Nat. Rev. Mol. Cell Biol.* **2009**, *10*, 659–671.
[12] a) J. S. Thrower, L. Hoffman, M. Rechsteiner, C. M. Pickart, *EMBO J.* **2000**, *19*, 94–102; b) S. K. Singh, I. Sahu, S. M. Mali, H. P. Hemantha, O. Kleifeld, M. H. Glickman, A. Brik, *JACS* **2016**, *138*, 16004–16015; c) N. Shabek, Y. Herman-Bachinsky, S. Buchsbaum, O. Lewinson, M. Haj-Yahya, M. Hejjaoui, H. A. Lashuel, T. Sommer, A. Brik, A. Ciechanover, *Mol. Cell* **2012**, *48*, 87–97; d) H. Sun, S. M. Mali, S. K. Singh, R. Meledin, A. Brik, Y. T. Kwon, Y. Kravtsova-Ivantsiv, B. Bercovich, A. Ciechanover, *Proc. Nat. Acad. Sci.* **2019**, *116*, 7805–7812; e) J. Lutz, E. Höllmüller, M. Scheffner, A. Marx, F. Stengel, *Angew. Chem. Int. Ed.* **2020**, *59*, 12371–12375.
[13] F. E. Reyes-Turcu, J. R. Shanks, D. Komander, K. D. Wilkinson, *J. Biol. Chem.* **2008**, *283*, 19581–19592.
[14] a) S. M. Nijman, M. P. Luna-Vargas, A. Velds, T. R. Brummelkamp, A. M. Dirac, T. K. Sixma, R. Bernards, *Cell* **2005**, *123*, 773–786; b) D. Komander, M. J. Clague, S. Urbé, *Nat. Rev. Mol. Cell Biol.* **2009**, *10*, 550–563.
[15] a) S. Eger, M. Scheffner, A. Marx, M. Rubini, *JACS* **2010**, *132*, 16337–16339; b) N. D. Weikart, H. D. Mootz, *ChemBioChem* **2010**, *11*, 774–777; c) T. Schneider, D. Schneider, D. Rösner, S. Malhotra, F. Mortensen, T. U. Mayer, M. Scheffner, A. Marx, *Angew. Chem. Int. Ed.* **2014**, *53*, 12925–12929.
[16] a) T. Schneider, A. Berg, Z. Ulusoy, M. Gamerdinger, C. Peter, M. Kovermann, *Sci. Rep.* **2019**, *9*, 1–18; b) T. Dresselhaus, N. D. Weikart, H. D. Mootz, M. P. Waller, *RSC Adv.* **2013**, *3*, 16122–16129; c) X. Zhao, M. Mißun, T. Schneider, F. Müller, J. Lutz, M. Scheffner, A. Marx, M. Kovermann, *ChemBioChem* **2019**, *20*, 1772–1777; d) G. Singh, S. Kumar, R. Das, *Anal. Chem.* **2023**, *95* (26), 10061–10067.
[17] a) X. Zhao, J. Lutz, E. Höllmüller, M. Scheffner, A. Marx, F. Stengel, *Angew. Chem. Int. Ed.* **2017**, *56*, 15764–15768; b) D. Rösner, T. Schneider, D. Schneider, M. Scheffner, A. Marx, *Nat. Protoc.* **2015**, *10*, 1594–1611.
[18] a) S. I. van Kasteren, H. B. Kramer, H. H. Jensen, S. J. Campbell, J. Kirkpatrick, N. J. Oldham, D. C. Anthony, B. G. Davis, *Nature* **2007**, *446*, 1105–1109; b) K. L. Kiick, E. Saxon, D. A. Tirrell, C. R. Bertozzi, *Proc. Nat. Acad. Sci.* **2002**, *99*, 19–24.
[19] a) R. Huisgen, *Angew. Chem. Int. Ed. Engl.* **1963**, *2*, 565–598; b) V. V. Rostovtsev, L. G. Green, V. V. Fokin, K. B. Sharpless, *Angew. Chem.* **2002**, *114*, 2708–2711.
[20] a) C. A. Castañeda, T. R. Kashyap, M. A. Nakasone, S. Krueger, D. Fushman, *Structure* **2013**, *21*, 1168–1181; b) C. A. Castañeda, A. Chaturvedi, C. M. Camara, J. E. Curtis, S. Krueger, D. Fushman, *Phys. Chem. Chem. Phys.* **2016**, *18*, 5771–5788.
[21] L. Jin, A. Williamson, S. Banerjee, I. Philipp, M. Rape, *Cell* **2008**, *133*, 653–665.
[22] D. K. Wilkins, S. B. Grimshaw, V. Receveur, C. M. Dobson, J. A. Jones, L. J. Smith, *Biochemistry* **1999**, *38*, 16424–16431.
[23] a) See Ref [16d]; b) A. Bremm, D. Komander, *Trends Biochem. Sci.* **2011**, *36*, 355–363; c) G. Dittmar, K. F. Winklhofer, *Front. Chem.* **2020**, *7*, 915; d) M. Akutsu, I. Dikic, A. Bremm, *J. Cell Sci.* **2016**, *129*, 875–880.
[24] a) S. Berger, S. Braun, *200 and more NMR experiments*, Wiley-Vch Weinheim, **2004**; b) J. A. Jones, D. K. Wilkins, L. J. Smith, C. M. Dobson, *J. Biomol. NMR* **1997**, *10*, 199–203; c) F. Delaglio, S. Grzesiek, G. W. Vuister, G. Zhu, J. Pfeifer, A. Bax, *J. Biomol. NMR* **1995**, *6*, 277–293; d) B. A. Johnson, R. A. Blevins, *J. Biomol. NMR* **1994**, *4*, 603–614.

Manuscript received: September 29, 2023
Revised manuscript received: November 17, 2023
Accepted manuscript online: November 20, 2023
Version of record online: November 30, 2023